Optical Materials 35 (2013) 366–371

Contents lists available at SciVerse ScienceDirect

Optical Materials

journal homepage: www.elsevier.com/locate/optmat

Dynamic characterization of photo-alignment of azo-dye-doped polymer using phase modulated polarimetry

Chun-I Chuang [a,*], Shiuan-Huei Lin [b], Yu-Faye Chao [a]

[a] Department of Photonics and Institute of Electro-Optical Engineering, National Chiao Tung University, 1001 University Rd., Hsinchu 30010, Taiwan, ROC
[b] Department of Electrophysics, National Chiao Tung University, 1001 University Rd., Hsinchu 30010, Taiwan, ROC

ARTICLE INFO

Article history:
Received 16 July 2012
Received in revised form 11 September 2012
Accepted 11 September 2012
Available online 23 October 2012

Keywords:
Anisotropic refractive index ellipsoid
Phase modulated polarimetry
Azo-benzene
Photo-induced molecular reorientation

ABSTRACT

Using a combination of two-probe-beam phase modulated polarimetry and a waveform extraction technique, we show it is possible to determine all the optical parameters of an anisotropic medium. Particularly, we have measured the dynamic changes of refractive index ellipsoid of the disperse red 19-doped poly(methyl methacrylate) under the irradiation of linear polarized lights. The long axis of the trans molecule can be aligned to the propagation direction of P-polarized light while it is irritated by two crossed polarized lights. The refractive indices and orientation angles can be determined in one cycle of modulation (20 μs) with sufficient precision of 10^{-6} and 0.1°, respectively. This work shows a new way to simultaneously monitor and control the photo-alignment process of azobenzene molecules in a polymer matrix.

1. Introduction

The photo-isomerization of azobenzene moiety can produce various types of molecular motions in their surroundings. Therefore, over the past decades, azobenzene-containing materials have attracted considerable attention in both scientific research areas and engineering applications. The molecular-scale photo-isomerization process can give rise to macroscopic photo-mechanical motions in the material systems, which recently are of great interest for the application in nanotechnology and light-driven biomolecular actuation [1–4]. In addition to acting as an efficient photo-switch [5–8], the photo-alignment of azobenzene derivatives with polarized light has been actively studied for various photonic applications, such as holography, nonlinear optics, and polarization sensitive optical elements [9–13]. For such applications, it is necessary to monitor the dynamic changes for the precise control; these photo control and measurement techniques can optimize both fabrication and performance of devices.

It is well known in azobenzene photo-chemistry that the azobenzene derivatives are usually in the rod shaped structure; these molecules will undergo the cycle of trans → cis → trans photo-isomerization when irradiated by the polarized light and then subsequently change their orientation [14]. The energy absorbed by azo-dye molecules for isomerization is proportion to the intensity and the cosine square of the angle between the transition dipole moment and the electric field direction of the exciting light. This mechanism is known as angular hole burning (AHB) [15,16]. In the azo-dye material systems, not only the photo-isomerization process, the vibration [17] and dipole–dipole interaction between the molecules [18,19] are also important. Under room temperature, the vibration and dipole–dipole interaction mechanisms can be neglected for a sample doped with low concentration of chromophores and exposed to a low power visible light. So, we only consider the photo-isomerization process in this work. Upon linear polarized irradiation, the photo-isomerization reaction cycle will continue until the dipole moment of the azobenzene molecule (which is usually along to the long axis of trans form) is perpendicularly aligned to the polarization direction of the inducing beam, as shown in Fig. 1. Thus, during photo-irradiation, the direction distribution of azo-dye molecules will gradually be transformed from randomness to a partially orderly fashion and then azo-dye-doped materials become optically anisotropic medium. Obviously, by introducing additional polarized beams to provide extra constrains, we can increase the population of ordered molecules to improve the performance of devices. Here, we conduct a four-irradiation-stage optical experiment by using two mutually incoherent orthogonally-polarized laser beams to irradiate the Dispersed-Red 19 azobenzene molecules doped poly(methyl methacrylate) (DR19-doped PMMA) polymer. Through this four-irradiation-stage process, we can clearly observe the stepwise increment in its birefringence.

To monitor the dynamics of photo-alignment of azo-dye molecules, it will be very powerful if one not only can measure the

* Corresponding author. Tel.: +886 3 5712121x56341; fax: +886 3 5735601.
E-mail address: chun.i.chuang@gmail.com (C.-I. Chuang).

0925-3467/$ - see front matter © 2012 Elsevier B.V. All rights reserved.
http://dx.doi.org/10.1016/j.optmat.2012.09.026

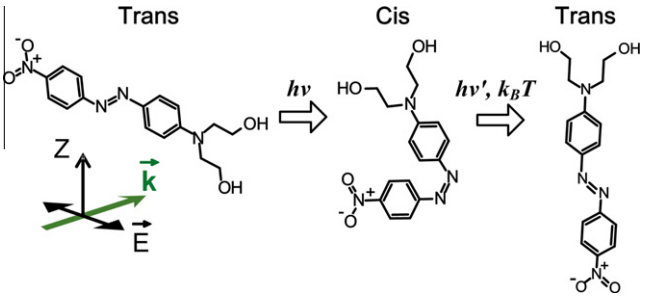

Fig. 1. Schematic of photo-isomerization process of DR19 under photo-irradiation by linear polarized light. After the dynamic equilibrium has been reached, the long axis of trans isomer is perpendicularly aligned to the polarization direction ($\vec{E}$) of the inducing beam, i.e. in the k–Z plane.

change of birefringence but also can determine the three principal refractive indices and orientations of the optical axis (hereafter, named as optical parameters, Ops) under photo-induced process. To our knowledge, this is the first study of measuring the dynamic process of the refractive index ellipsoid. Furthermore, we showed that the direction of azo-dye molecules can be optically controlled from a plane to a line distribution. In this work, we propose to conduct a two-probe-beam phase modulated polarimetry to monitor all above mentioned Ops of material during irradiation by a novel waveform extraction technique. In previous study [20] of the one-probe-beam phase modulated polarimetry, we have applied lockin amplifier option in the data acquisition (DAQ) system and resolved the magnitude of birefringence (Δn) better than 10^{-6} for a thick medium. For the two-probe-beam system, instead of using the option of lockin amplifier in DAQ, we record the digitized oscilloscopic waveforms of temporal transmitted intensity for both Fourier and waveform extraction methods. In addition to extracting the Ops by fitting the theoretical waveform to the measured waveform, which is named as waveform extraction technique in this article, we also use the conventional Fourier transformation of the recorded waveform to decouple the thickness from the Ops. By combining both techniques, we can rapidly and simultaneously determine all the Ops.

2. Fundamentals for determining the optical parameters

Recently [20], we have obtained the photo-induced phase retardation and the azimuth angle of optical axis (OA) by a one-probe-beam phase modulated polarimetry. In the laboratory coordinate system, we like to understand the relative motion of the refractive index ellipsoid of azo-dye-doped polymer while it is under irradiation. So, we establish a two-probe-beam configuration, as in Fig. 2, to measure the irradiated DR19-doped PMMA block. According to the definition of Euler angles in mathematics, the laboratory coordinates X, Y, and Z, are used to describe the propagation of light and the reference of three principal axes PA_1, PA_2, and PA_3, where the X–Y plane is defined as the incident plane, as shown in the lower part of Fig. 2. A biaxial medium is comprised by three principal refractive indices, n_1, n_2, and n_3 at three corresponding orthogonal axes PA_1, PA_2, and PA_3. The three Euler angles η, φ and ξ are defined as the relation between (PA_1, PA_2, PA_3) and (X, Y, Z) by X–Z–X extrinsic rotations [21]. In this work, we can measure the dynamic changes of Ops (n_1, n_2, n_3, η, φ and ξ) in a photo-induced process.

The temporal intensity can be obtained by the production of Jones matrix and expressed as

$$I_j(\vec{v}, \Delta_p(t)) = I_{0j}[A - D\cos 2\Psi_{effj} - (B + F\sin 2\Psi_{effj}\sin\Delta_{effj}) \times \cos\Delta_p + (C + B\sin 2\Psi_{effj}\sin\Delta_{effj})\sin\Delta_p], \quad (1)$$

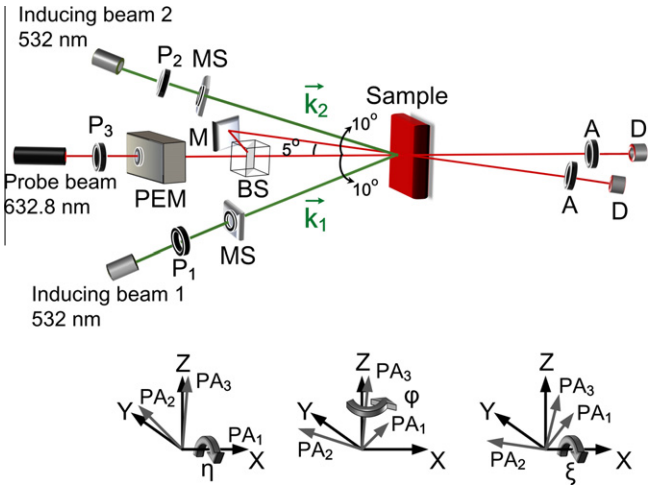

Fig. 2. Schematic setup of a two-probe-beam phase modulated polarimetry for probing the photo-induced processes. The probe system uses a HeNe laser (632.8 nm), and consists of a polarizer (P_3), a photoelastic modulator (PEM), a beam splitter (BS), a mirror (M), two analyzers (A) and two photo diode detectors (D). There are also two inducing beams using lasers of orthogonal polarization states (P and S) at $\lambda = 532$ nm. P_1 and P_2 denote polarizers, and MS denotes mechanical shutter. The lower part is the Euler angles (η, φ, ξ) between the propagation axes (X, Y, Z) and material axes (PA_1, PA_2, PA_3) by X–Z–X extrinsic rotations.

where

$$\begin{aligned}
A &= t_{ppj}(\bar{t}_{ppj} + \bar{t}_{spj}) + t_{psj}(\bar{t}_{psj} + \bar{t}_{ssj}) + t_{spj}(\bar{t}_{ppj} + \bar{t}_{spj}) + t_{ssj}(\bar{t}_{psj} + \bar{t}_{ssj}) \\
B &= t_{ppj}(\bar{t}_{psj} + \bar{t}_{ssj}) + t_{psj}(\bar{t}_{ppj} + \bar{t}_{spj}) + t_{spj}(\bar{t}_{psj} + \bar{t}_{ssj}) + t_{ssj}(\bar{t}_{ppj} + \bar{t}_{spj}) \\
C &= i[-t_{ppj}(\bar{t}_{psj} + \bar{t}_{ssj}) + t_{psj}(\bar{t}_{ppj} + \bar{t}_{spj}) - t_{spj}(\bar{t}_{psj} + \bar{t}_{ssj}) + t_{ssj}(\bar{t}_{ppj} + \bar{t}_{spj})] \\
D &= t_{ppj}(\bar{t}_{ppj} + \bar{t}_{spj}) - t_{psj}(\bar{t}_{psj} + \bar{t}_{ssj}) + t_{spj}(\bar{t}_{ppj} + \bar{t}_{spj}) - t_{ssj}(\bar{t}_{psj} + \bar{t}_{ssj}) \\
F &= i[t_{ppj}(\bar{t}_{psj} + \bar{t}_{ssj}) - t_{psj}(\bar{t}_{ppj} + \bar{t}_{spj}) + t_{spj}(\bar{t}_{psj} + \bar{t}_{ssj}) - t_{ssj}(\bar{t}_{ppj} + \bar{t}_{spj})].
\end{aligned} \quad (2)$$

The phase of photoelastic modulator (PEM), Δ_p, is modulated with amplitude and frequency at δ_0 and ω, respectively. The operation frequency of PEM is 50 kHz, so within 20 μs, the two intensity waveforms at different incident angles can be simultaneously recorded for extracting the Ops, as shown in Fig. 3. The subscript $j = 1, 2$ denotes the incident angle θ_{ij} of the two probe beams. The Ψ_{effj} and Δ_{effj} are the effective ellipsometric parameters of beam splitter (BS) and the combination of BS and mirror (M), respectively. If the subscripts P and S are the polarized light parallel and perpendicular to the incident plane, respectively; then t_{mn}, ($\vec{v}$) is the corresponding Fresnel transmission coefficients of its polarization state. The six Ops (n_1, n_2, n_3, η, φ and ξ, noted as $\vec{v}$) and the thickness are implicitly contained in the transmission coefficients [22]. Therefore, one can determine these parameters by fitting the theoretical model to the measured waveforms. In the numerical procedure, the goodness-of-fit can be evaluated by the reduced chi square (RCS) [23], which is defined as

$$RCS = \frac{1}{N - M - 1}\sum_{\theta_{ij}}\sum_{t}\frac{\{I(\vec{v}, \Delta_p(t))_{calc} - I(\vec{v}, \Delta_p(t))_{exp}\}^2}{\delta I(\vec{v}, \Delta_p(t))^2_{exp}}, \quad (3)$$

The parameters N and M are the number of data points and variables, respectively, and $\delta I(\vec{v}, \Delta_p(t))_{exp}$ denotes the standard deviation. Through the genetic algorithm (GA) [24], the Ops can be obtained in a short time without being trapped in the local minimum.

For extracting the Ops of sample by GA, we have to determine the thickness by combining the Fourier transform technique in the one-probe-beam configuration. First, we roughly measured

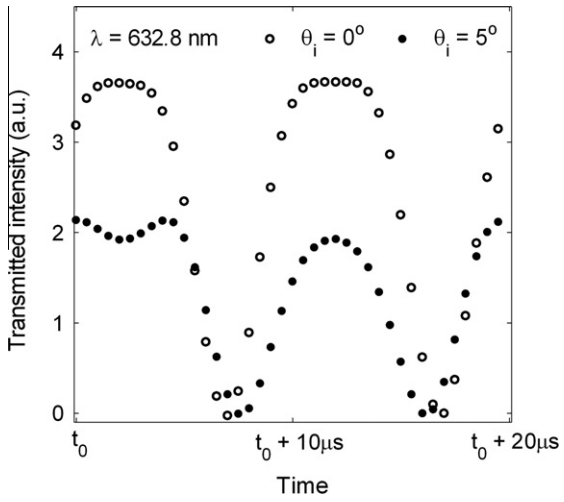

Fig. 3. One cycle (20 μs) of temporal intensity waveforms measured by a two-probe-beam phase modulated polarimetry. These two waveforms were simultaneously acquired, allowing for extracting all the optical parameters of our DR19-doped PMMA sample. Here, θ_i: incident angle; hollow circles (○): $\theta_i = 0°$ and solid circles (●): $\theta_i = 5°$. t_0 is the initial time of measurement, here $t_0 = 2699.9$ s (end of stage 2).

the thickness of sample by a micrometer as d_1 considered as known in GA of waveform extraction for Δn; then solve the thickness d_2 from its phase retardation ($\Delta_Q = 2\pi\Delta nd/\lambda$), which was determined by the ratio of Fourier components [20]. These determination cycles have been repeatedly executed until the difference of thickness between two adjoint cycles converges to 1 nm.

3. Experiments

3.1. Sample preparation

Our poly(methyl methacrylate) (PMMA) host matrix was made from the chain reaction of polymerization of methyl methacrylate (MMA) (Lancaster) monomers by use of a thermal initiator, azobisisobutyronitrile (AIBN) (Showa). To preserve the uniformity of the refractive index inside the thick sample we made the polymer blocks in two stages at different temperatures [25]. In the first step, the initiator, AIBN, (~0.5 wt.%) and disperse red 19 (DR19) (Aldrich) molecules (~0.5 wt.%) are dissolved in solvent MMA. The solution was purified to remove the un-dissolved particles so as to reduce light scattering centers. The purified solution was poured into a square glass tube and then put in a pressure chamber at room temperature for about 120 h until the solution turned into homogeneously viscid. In the second step, the temperature of the chamber was elevated to 45 °C for 24 h to accelerate the thermo-decomposition rate of AIBN. Chain reaction was accelerated until polymerization was completed and the sample became a self-sustaining slab bulk with dimensions of $10 \times 10 \times 1.8$ mm^3. This is named as DR19-doped PMMA polymer.

3.2. Optical experiments

The dynamics of the photo-alignments of DR19 azobenzene molecules in the polymer matrix were characterized by a two-probe-beam phase modulated polarimetry, in which two beams were incident at different angles. Through the GA, the Ops can be precisely determined by fitting the theoretical model to the measured waveforms. The optical setup of the two-probe-beam phase modulated polarimetry is shown in Fig. 2. We like to emphasize that the two inducing beams are mutually incoherent orthogonally-polarized beams from two laser diodes at 532 nm. The probe beam is a HeNe laser at 632.8 nm (40 mW/cm^2), where DR19-doped PMMA exhibits very low absorption [26]. The two-probe-beam system consists of the linear polarized light with azimuth angle at −45° passing through the PEM (PEM 90, Hinds), whose modulation axis is set at 0° to the incident plane. Then the modulated beam passes to the BS and M for the two modulated probe beams. These two beams are separately transmitted through the photo-sensitive medium, one is in normal and the other is offset by 5°. The effects of BS and M in the system have been well calibrated by a modified three intensity technique [27]. There are two analyzers in the probe system, both transmission axes of which are set at 45°, and then the two modulated waveforms are simultaneously acquired by a 10 MHz DAQ system. Both waveforms are measured within 20 μs, from which the Ops can be extracted through the GA.

For characterizing the dynamics of photo-alignment of azo-dye molecules in polymer matrix, we conduct a four-irradiation-stage process on the sample. The two inducing beams come from two independent laser diodes at 532 nm to avoid the interference. The intensity fluctuation of the inducing beams can be stabilized within ±3% after 1.5 h, and then the intensities of both inducing beams are attenuated to be 4.7 mW/cm^2 in order to reduce the photo-thermal effect in refractive index [28]. These two beams are linear polarized, one is parallel (inducing beam 1: P-polarized) and the other is perpendicular (inducing beam 2: S-polarized) to the incident plane. The incident angles of both beams are set at 10° and −10° with respect to the sample normal. The irradiation time for both inducing beams can be controlled by two mechanical shutters (MSs). In order to demonstrate the dynamic changes of the principal refractive indices as well as the Euler angles of the azo-dye-doped material, we sequentially applied four stages of photo-induced process: (1) without any inducing beam for 5 min; (2) turn on the P-polarized light for 40 min; (3) turn on an extra S-polarized light for 40 min; in the end (4) turned off both inducing beams for 20 min.

For minimizing the thermal heating effect [28–31] in our experiment, all the four stages are conducted at room temperature (22.3 ± 0.2 °C). The beam profiles of both inducing and probe beams are measured by a CCD camera (F-032B, Pike; resolution: 640 × 480; resolution depth: 16 bits; frame rate: 208 fps). The beam profiles are averaged by 100 frames for display.

4. Results and discussion

Fig. 4 is the beam profiles of both inducing and probe beams measured by a CCD camera. Since the spot size of the inducing beam (1.35 mm) is only three times larger than that of the probe beam (0.45 mm), the measured intensity is the average value over the probe area. Therefore, the actual variation of refractive indices at the peak of inducing beam should be larger than the measured values.

The thickness of film dealt in ellipsometry/polarimetry is much smaller than the wavelength of probe beam [32,33], while this bulk medium is much thicker than wavelength. For extracting the 6 Ops of the bulk, we have to decouple the thickness in the intensity waveform prior to extract other Ops. The thickness of azo-dye-doped PMMA block measured by micrometer is 1800 ± 10 μm, which has been considered as constant for the preliminary cycle of the decoupling process. In this experiment, Δ_Q has been saturated to be 20.52° when irradiated by the P-polarized light at the incident angle of 10°. Here, the thickness has been determined to be 1809.851 ± 0.001 μm after the repeated cycles. The shrinkage of our material can be neglected [25], therefore, the adopted thickness is 1809.851 μm for the determination of Ops by the waveform extraction technique at four stages of photo-induced process.

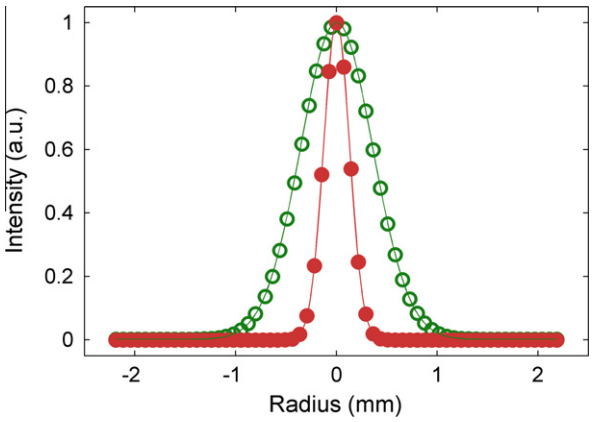

Fig. 4. Beam profiles of inducing and probe beams. Hollow circles (○): inducing beam and solid circles (●): probe beam.

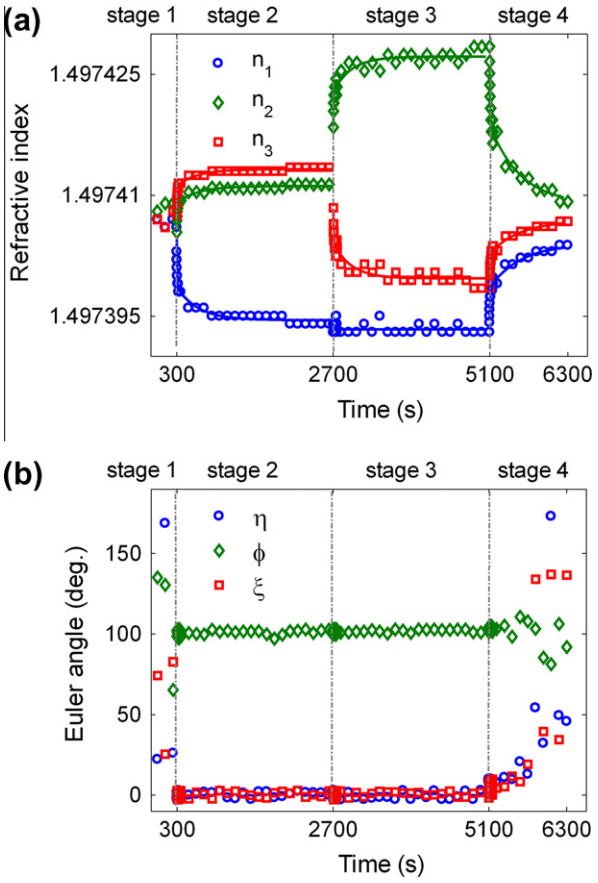

Fig. 5. Refractive index ellipsoid extracted from the measured intensity waveforms. The dynamics of (a) principal refractive indices and (b) Euler angles are obtained at four irradiation stages. Stage 1, t = 0–300 s: no inducing beam; stage 2, t = 300–2700 s: turn on the P-polarized beam; stage 3, t = 2700–5100 s: turn on the additional S-polarized beam; stage 4, t = 5100–6300 s: turn off both beams. The solid lines in (a) are obtained by fitting the biexponential functions of the three stages.

The dynamic changes of the Ops during the photo-isomerization have been resolved in this research. Not only the three principal refractive indices, but also the photo-alignments of the molecules are measured by the two-probe-beam polarimetry. The experimental results of the refractive indices and Euler angles of the three principal axes are shown in Fig. 5 for all the four photo-induced stages. For a legible figure, we display one data point/s in the beginning 1 min for stages 2, 3 and 4; otherwise, we only express one data point every 2 min. According to the results, the distribution of the azo-dye molecules and its corresponding effective refractive index ellipsoid can be illustrated in Fig. 6.

In stage 1: If there is no irradiation, the angular orientations of the azo-dye molecules are randomly distributed, and the effective refractive index ellipsoid is spherical, as shown in Fig. 6a. In the one-probe-beam phase modulated ellipsometry, we have accurately measured the refractive index of PQ-doped PMMA with precision of 10^{-3} [20]. In 2009 [34], Dubreuil et al. proved that both random and systematic errors can be reduced by performing the measurement at more than one output channels. So, a higher precision and accuracy can be expected by performing the measurement at two incident angles. This system obtains an averaged refractive index to be 1.497407 with the precision of 10^{-6}. According to Wu's [29] measured refractive indices of doped PMMA with various concentration of DR19 (3–15 wt.%) for different temperature (30–80 °C), we extrapolate from their results then obtain 1.4976 for the refractive index of our sample (0.5 wt.%, 22.3 °C), which is only 2×10^{-4} higher than our measured value.

In stage 2: Once the P-polarized light has been turned on, the long axes of trans isomers parallel to the pump polarization will absorb the energy, and then change to cis isomers. Since the cis isomers are unstable, they will convert back to trans isomers. Sekkat et al. [15] stated that the directions of trans isomers will tend to be conically distributed with a center line parallel to the direction of pump polarization. In macro scale, a negative uniaxial medium ($n_2 \sim n_3 > n_1$) has thus been induced by the P-polarized beam [35], such as shown in Fig. 6b. This phenomenon has been observed in the experiment, during irradiation, the sample stays as uniaxial medium, and its OA is in the same orientation (Fig. 5b). The OA of the sample is on PA_1, which is on the incident plane. The angle between axes X and the OA is equal to 101.7 ± 0.1°, so the OA is almost at the same direction of pump polarization. This photo-isomerization process will cause trans isomers to be accumulated on the PA_2–PA_3 plane, which is perpendicular to the pump polarization. In the end, the three principal refractive indices will reach to a dynamic equilibrium value, thus n_2 and n_3 are saturated to a larger value while n_1 decreases to a smaller value in comparison with the value before irradiation. Since the precision measurement of induced birefringence for a thick PQ-doped PMMA bulk can reach less than 10^{-6} by one-probe-beam phase modulated polarimetry [20], the order of 10^{-5} photo-induced birefringence ($\sim 1.5 \times 10^{-5}$) is resolvable by this technique. It is known the temperature do affect the refractive index [28,29], birefringence [28,30], and the reaction rate of the photo-isomerization [31] of the azo-dye-doped polymers under irradiation. Here, we are focusing our study in the orientation of the irradiated azo-dye molecules, so we choose a low concentration of DR19 (0.5 wt.%) doped in PMMA under a low-power (4.7 mW/cm^2) irradiation for this study. The glass transition temperature (T_g) of the sample is close to the pure PMMA, i.e. $T_g \sim 100$ °C, while the room temperature is much lower than T_g of this sample, therefore, the temperature effect on the refractive indices can be neglected.

In stage 3: An extra S-polarized light has been turned on for another 40 min. Similar isomerization process will redistribute the orientation direction of the molecules on the PA_2–PA_3 plane; the long axes of the rod-shaped molecules will be gradually oriented to the propagation direction of P-polarized light ($\sim PA_2$). Therefore, the refractive index n_2 increases to a higher value, but n_1 stays the same value as in stage 2, while n_3 decreases to the same quantity as n_1. Just as expected in the angular re-distribution theory [15,16], this sample does transform from a negative uniaxial to a biaxial medium by the extra S-polarized light. After the dynamic equilibrium has been approached, the sample will ultimately turn

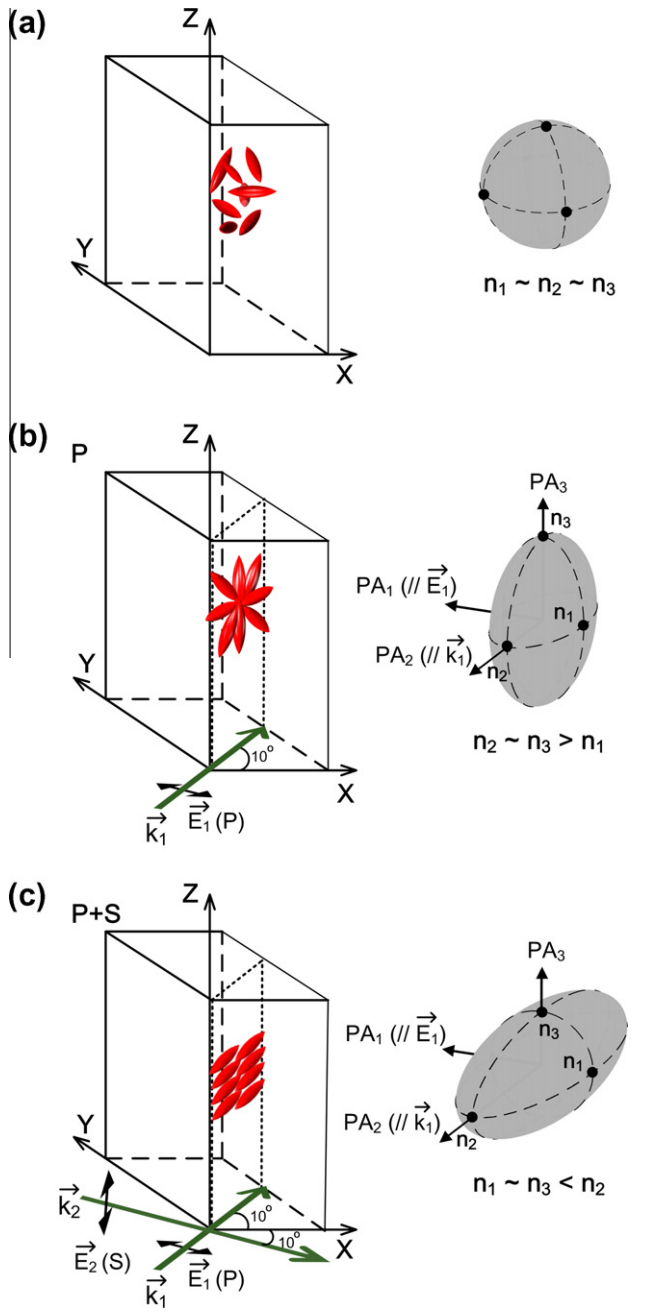

Fig. 6. Photo-isomerization processes under various irradiation conditions. (a): no irradiation; (b): P-polarized irradiation only and (c): combination of P- and S-polarized irradiations. The P and S inducing beams propagate along $\vec{k}_1$ and $\vec{k}_2$, respectively. Left part: orientations of the molecules; right part: the corresponding effective refractive index ellipsoid.

into a positive uniaxial (OA = PA_2) medium, as shown in Fig. 6c. The unexpected difference between n_1 and n_3 (in Fig. 5a) may be explained by the biaxial configuration on the surface of azo-dye-doped polymer [36]. The results clearly show that the azo-dye molecules can be further aligned by the extra polarized pump light, thus increase the number of ordered molecules and enhance the birefringence of the medium.

In the end stage: Turn off all pump lights, the orientation of the molecules will be randomized by rotational Brownian motion, known as rotational diffusion (RD) [15,16]. As a result, the sample will transform back to be an isotropic medium. The weak residual birefringence ($\sim 10^{-7}$) in the sample is the limitation of this measurement technique. So, the photo-isomerization of DR19 azobenzene molecules in PMMA polymer matrix is thermally reversible.

Table 1
Dynamical parameters of photo-induced reaction for different stages.[a]

	k_{ai} (s^{-1})	k_{bi} (s^{-1})	A_i ($\times 10^{-6}$)	B_i ($\times 10^{-6}$)	C_i
Stage 2 (induced by P-polarized light)					
n_1	0.171	0.003	6.0	4.1	1.4974046
n_2	0.183	0.003	−3.1	−2.0	1.4974060
n_3	0.171	0.003	−3.0	−2.1	1.4974082
Stage 3 (induced by P- and S-polarized light)					
n_1	–	–	–	–	–
n_2	0.19	0.004	−4.3	−4.4	1.4974185
n_3	0.189	0.004	4.3	4.4	1.4974084
Stage 4 (turn off both lights)					
n_1	0.085	0.002	−3.9	−5.5	1.4973946
n_2	0.084	0.002	7.2	9.9	1.4974259
n_3	0.085	0.002	−3.0	−4.2	1.4973997

[a] The subscript i = 1, 2, 3 denotes the three principal axes.

The biexponential function of the growth and decay processes of the refractive index can be used to express the photo-induced process quantitatively. The typical biexponential function is expressed as:

$$n_i = A_i \exp(-k_{ai}t) + B_i \exp(-k_{bi}t) + C_i, \quad (4)$$

where n_i is the measured refractive indices at time t, and the subscript i = 1, 2, 3 denotes the three principal axes; k_{ai} and k_{bi} represent the reaction rate with amplitudes A_i and B_i; constant C_i is the offset of the function. The photo-induced reaction for growth or decay process of DR19-doped PMMA are obtained from fitting the biexponential function to our measurements; the reaction rates and the corresponding amplitudes of each stage are listed in Table 1, and the fitted curves (solid lines) are plotted in Fig. 5a. In stage 2, the amplitudes of the dynamic change in n_1 (A_1 and B_1) are twice of those in n_2 and n_3. This consists with the theoretical model of photoisomerization, the dye molecules, fixed in a solid matrix, preferentially absorb light polarized along their transition moment. In stage 3, both reaction rates are the same, while their amplitudes are doubled in comparison with the values in stage 2. Song et al. [30] also showed that the reaction rates are independent of the power of inducing beam when the operation temperature is below T_g, however, the amplitudes do depend on the pump power. In stage 4, the reaction rates of both fast and slow processes are half of those in stages 2 and 3, which means the relaxation process is slower than pump process.

5. Conclusions

After decoupling the thickness of the sample by the combination of waveform extraction and Fourier transform techniques, in this two-probe-beam phase modulated polarimetry, we have demonstrated that one can monitor the dynamic changes of all the Ops (three principal refractive indices and its Euler angles) of the DR19-doped PMMA during irradiation processes. A 50 kHz data acquisition speed can be reached; the precisions of the system are 10^{-6} and 0.1° for the refractive indices and principal angles of refractive index ellipsoid, respectively. According to the angular hole burning concept, these results can be used to identify the dynamics of photo-alignment in DR19-doped PMMA polymer matrix. Comparing with the conventional photo-induced birefringence measurement in azo-dye-doped polymer, this method provides a clearer picture of the molecular motions with respect to the laboratory coordinates under the photo-isomerization. In these controlled irradiation processes, one can observe the variation of birefringence in the polymer because the directions of trans isomers have

been re-oriented from random to a plane then to a line distribution. Thus, we can conclude that the modifications of the refractive indices are caused by increasing the aligned molecules according to the polarization states of the pump beams and their propagation directions. Additionally, the biexponential growth and decay in the refractive indices suggest that both fast and slow processes exist during the photo-alignment of DR19 azo-dye molecules by using polarized light. This study provides a new approach to simultaneously monitor and control the direction of azo-dye molecules for further photonic applications, such as holographic data storage and photo-switch. Fig. 6 shows that it is possible to optically manipulate the orientation of molecules in order to enhance the diffraction efficiency of a grating. In our future work, we like to apply the stroboscopic illumination technique [37] to establish an imaging polarimetry for measuring the dynamic properties of the photorefractive medium.

Acknowledgements

The authors acknowledge the funding from National Science Council of Taiwan under the Grant of NSC98-2221-E-009-024 and NSC100-2112-M-009-005. We also appreciate Professor Shawn-Yu Lin and Mei-Li Hsieh for their valuable suggestions. Shawn-Yu Lin, Distinguished Professor of the Future-Chips Constellation and Department of Physics, Rensselaer Polytechnic Institute; Mei-Li Hsieh, Professor of the Department of Photonics, National Chiao Tung University.

References

[1] E.D. King, P. Tao, T.T. Sanan, C.M. Hadad, J.R. Parquette, Org. Lett. 10 (2008) 1671–1674.
[2] M. Zhou, X. Liang, T. Mochizuki, H. Asanuma, Angew. Chem. 122 (2010) 2213–2216.
[3] A.A. Beharry, L. Wong, V. Tropepe, G.A. Woolley, Angew. Chem. Int. Ed. 50 (2011) 1325–1327.
[4] O. Berthoumieu, A.V. Patil, W. Xi, L. Aslimovska, J.J. Davis, A. Watts, Nano Lett. 12 (2012) 899–903.
[5] K.G. Yager, C.J. Barrett, J. Photochem. Photobiol. A 182 (2006) 250–261.
[6] M. Böckmann, N.L. Doltsinis, D. Marx, Phys. Rev. E 78 (2008) 036101.
[7] A.A. Beharry, O. Sadovski, G.A. Woolley, J. Am. Chem. Soc. 133 (2011) 19684–19687.
[8] J. Mysliwiec, M. Ziemienczuk, A. Miniewicz, Opt. Mater. 33 (2011) 1382–1386.
[9] A.G. Chen, D.J. Brady, Opt. Lett. 17 (1992) 441–443.
[10] R. Raschellà, I.-G. Marino, P.P. Lottici, D. Bersani, A. Lorenzi, A. Montenero, Opt. Mater. 25 (2004) 419–423.
[11] H. Ono, A. Hatayama, A. Emoto, N. Kawatsuki, Opt. Mater. 30 (2007) 248–254.
[12] L.M. Goldenberg, L. Kulikovsky, Y. Gritsai, O. Kulikovska, J. Tomczyk, J. Stumpe, J. Mater. Chem. 20 (2010) 9161–9171.
[13] N. Tsutsumi, Y. Nagano, J. Opt. Soc. Am. B 29 (2012) 23–28.
[14] G.S. Kumar, D.C. Neckers, Chem. Rev. 89 (1989) 1915–1925.
[15] Z. Sekkat, J. Wood, W. Knoll, J. Phys. Chem. 99 (1995) 17226–17234.
[16] J.A. Delaire, K. Nakatani, Chem. Rev. 100 (2000) 1817–1845.
[17] A. Natansohn, P. Rochon, X. Meng, C. Barrett, T. Buffeteau, S. Bonenfant, M. Pézolet, Macromolecules 31 (1998) 1155–1161.
[18] A. Migalska-Zalas, Z. Sofiani, B. Sahraoui, I.V. Kityk, S. Tkaczyk, V. Yuvshenko, J.-L. Fillaut, J. Perruchon, T.J.J. Muller, J. Phys. Chem. B 108 (2004) 14942–14947.
[19] D. Apitz, R.P. Bertram, N. Benter, W. Hieringer, J.W. Andreasen, M.M. Nielsen, P.M. Johansen, K. Buse, Phys. Rev. E 72 (2005) 036610.
[20] C.I. Chuang, Y.N. Hsiao, S.H. Lin, Y.F. Chao, Opt. Commun. 283 (2010) 3279–3283.
[21] J.G. Papastavridis, Analytical Mechanics, Oxford, New York, 2002, (Chapter 1).
[22] I.J. Hodgkinson, Q.H. Wu, Birefringent Thin Films and Polarizing Elements, World Scientific, Singapore, 1997.
[23] G.E. Jellison Jr., Appl. Opt. 30 (1991) 3354–3360.
[24] J.H. Holland, Adaptation in Natural and Artificial Systems, MIT Press, Cambridge, 1992.
[25] S.H. Lin, K.Y. Hsu, W.Z. Chen, W.T. Whang, Opt. Lett. 25 (2000) 451–453.
[26] F.X. Qiu, D.Y. Yang, P.P. Li, X. Wang, Express Polym. Lett. 2 (2008) 823–828.
[27] Y.F. Chao, K.Y. Lee, Y.D. Lin, Appl. Opt. 45 (2006) 3935–3939.
[28] J.J. Park, Photo-induced molecular reorientation and photothermal heating as mechanisms of the intensity-dependent refractive index in dye-doped polymers, PhD thesis, Washington State University, Pullman, WA, 2006.
[29] S. Wu, F. Zeng, H. Wang, W. She, Z. Cai, J. Appl. Polym. Sci. 89 (2003) 2374–2377.
[30] O.-K. Song, C.H. Wang, M.A. Pauley, Macromolecules 30 (1997) 6913–6919.
[31] H. Ono, N. Kowatari, N. Kawatsuki, Opt. Mater. 15 (2000) 33–39.
[32] G.H. Bu-Abbud, N.M. Bashara, Appl. Opt. 20 (1981) 3020–3026.
[33] D. Pristinski, V. Kozlovskaya, S.A. Sukhishvili, J. Opt. Soc. Am. A 23 (2006) 2639–2644.
[34] M. Dubreuil, S. Rivet, B.L. Jeune, J. Cariou, Appl. Opt. 48 (2009) 6501–6505.
[35] O. Yaroshchuk, T. Sergan, J. Kelly, I. Gerus, Jpn. J. Appl. Phys. 41 (2002) 275–279.
[36] A.D. Kiselev, V. Chigrinov, D.D. Huang, Phys. Rev. E 72 (2005) 061703.
[37] C.Y. Han, Y.F. Chao, Rev. Sci. Instrum. 77 (2006) 023107.